JANUARY 1990 VOL 24 No 1

CARDIOVASCULAR RESEARCH

BRITISH MEDICAL ASSOCIATION TAVISTOCK SQUARE LONDON WC1H 9JR

CARDIOVASCULAR RESEARCH

Published monthly in association with the British Cardiac Society

Cardiovascular Research is a journal concerned with the link between the basic sciences, clinical physiology and clinical cardiology. Thus its purpose is to provide a forum for those engaged in the application of methods of the basic sciences to the understanding of clinical disease. The formulation of animal models of disease constitutes an important and major area of interest, but not to the exclusion of other subjects. Papers on clinical topics or having a wholly basic scientific content will be accepted, as will review articles on topics of current interest or disease processes. The only criteria for acceptance will be relevance to cardiovascular topics and scientific quality.

Submission of a paper will be held to imply that it contains original work which has not been published before and is not being submitted for publication elsewhere. Permission to reproduce in whole or in part must be obtained from the publisher.

Contributors should send *two* copies of the text, references, tables, and figures. Manuscripts must be typewritten, on one side of the paper in double space with wide margins. The following information should be given on a single separate sheet: (1) title and a short title for the running head; (2) authors' names and affiliations; (3) department in which the work was done. Footnotes, on the same sheet, should list: (i) the authors' present addresses if different from the departments in which the work was done; (ii) name and address of author to whom correspondence and reprint requests should be addressed; (iii) receipt of grants. A concise and informative structural abstract should be provided.

Correspondence Letters containing critical assessments of material published in *Cardiovascular Research,* including reviews, will be considered for publication. They should be sent to the Editor within 6 months of the appearance of the article concerned.

Rapid publication Short papers will be considered for rapid publication (within 3 months). These should contain material which merits accelerated publication and must not occupy more than 4 journal pages, including tables, figures and references (authors are responsible for assessing the length accurately before submission). Current standard section headings should be used. Abstracts should not exceed 100 words, and there should not be more than 10 references. Papers submitted for rapid publication should be clearly marked as such. Rejection does not preclude resubmission as a full paper. No proofs will be sent, so the submitted copy must be entirely correct.

Instructions to authors. These are printed in full annually in the January issue. The following should act as a guide, but authors are urged to consult the full instructions as papers that do not comply will be returned for revision.

SI Units All units of measurement, except for blood pressures, should be in SI (including those in the figures). Blood pressures should be expressed in mm Hg.

References should be typed (double spacing) on separate sheets. Contributors are responsible for the accuracy of their references. The *numerical* system is used, and references should appear in the numerical order in which they are first cited in the text and should be in the Vancouver style. Journal titles should be abbreviated in accordance with the style of *Index Medicus.*

Illustrations Half tones should be presented as unmounted, glossy prints and should be clearly identified on the back of the photograph. Photocopies of line drawings are acceptable. Figures should be numbered consecutively in Arabic numerals. Legends should be typed (double spacing) on separate sheets. Colour illustrations can be reproduced at the author's cost.

Tables should be typed on separate sheets and numbered consecutively in Roman numerals. Tables should be kept to a minimum. Material which is not subsequently commented upon in the text should *not* be included in the tables.

Proofs Proofs will be sent to the author (except for rapid communications). Corrections other than printer's errors may be charged to the author.

Reprints Reprints are available on payment of the necessary costs if they are ordered when the proof is returned.

Notice to advertisers Applications for advertisement space and rates should be made to the Advertisement Manager, *Cardiovascular Research,* BMA House, Tavistock Square, London WC1H 9JR.

Notice to subscribers

Cardiovascular Research is published monthly. The annual subscription rates are £129 inland and £153 overseas (USA $248). Combined rate: *British Heart Journal* & *Cardiovascular Research* £200 inland and £233 overseas (USA $385). Orders should be sent to the Subscriptions Manager, *Cardiovascular Research,* BMA House, Tavistock Square, London WC1H 9JR. Orders can also be placed with any leading subscription agent or bookseller. (For the convenience of readers in the USA, subscription orders, with or without payment, may also be sent to: *British Medical Journal,* Box 560B, Kennebunkport, Maine 04046. Inquiries must, however, be addressed to the publisher in London. All inquiries regarding air mail rates and single copies already published should be addressed to the publisher in London. Application to mail at second class postage rate is pending at Rahway NJ Postmaster. Send address changes to: Cardiovascular Research, c/o Mercury Airfreight International Ltd Inc, 2323 Randolph Avenue, Avenel, NJ 07001, USA.)

Papers for publication should be sent to the Editor, *Cardiovascular Research,* c/o University Department of Physiology, Parks Road, Oxford OX1 3PT. Queries about submitted manuscripts should be addressed to Miss Christine Lake, at the above address (Tel: 0865 310691; FAX 0865 272469). Address queries about accepted manuscripts to Dr Oliver Brooke, 49 Rusholme Rd, London SW15 3LF (Tel: 01 788 2228). The Editor does not accept responsibility for damage to or loss of papers submitted.

ISSN 0008 6363

CONTENTS

No 1 JANUARY 1990

No 2 FEBRUARY 1990

No 3 MARCH 1990

No 4 APRIL 1990

No 5 MAY 1990

No 6 JUNE 1990

No 7 JULY 1990

No 10 OCTOBER 1990

No 11 NOVEMBER 1990

No 12 DECEMBER 1990

Acute pulmonary microembolism induces different regional changes in preload and contraction pattern in canine right ventricle

Bernhard Zwissler, Helmuth Forst, Konrad Messmer

Abstract

Study objective – **The aim of the study was to investigate the influence of acute pulmonary embolism on local myocardial preload and contraction pattern in right ventricle.**

Design – **Measurements of preload and contraction pattern were made in inflow and outflow tracts of canine right ventricular free wall by sonomicrometry. Local right ventricular preload was assessed from end diastolic segment length. Contraction pattern was assessed from pressure-length loops and quantified by calculating maximal, systolic, and postsystolic shortening, and protosystolic segment elongation. Data were obtained before and after microembolisation with 100 μm glass beads in combination with oleic acid.**

Subjects – **13 foxhounds of either sex were used, weight 20.4±4.0 kg.**

Measurements and main results – **Pulmonary microembolisation resulted in a rise in systolic, mean, and end diastolic right ventricular pressure and pulmonary vascular resistance. At the same time, the pressure-length loops, originally triangular or oval, became rectangular in both inflow and outflow tract. Normalised end diastolic segment length increased in the inflow tract from 10.0 to 10.3 mm ($p<0.01$), but simultaneously decreased in the outflow tract, from 10.0 to 9.6 mm ($p<0.05$). Segment shortening in the inflow tract was not affected but deteriorated in the outflow tract from 11.6 to 2.7% ($p<0.01$).**

Conclusions – **Increase in afterload due to pulmonary microembolisation caused regionally different changes in local preload and segment shortening in right ventricular free wall. Clinically available measures of global right ventricular preload do not assess these local differences in preload and therefore may fail to reflect the functional state of the right ventricle accurately.**

Department of Experimental Surgery, University of Heidelberg, Im Neuenheimer Feld 347, 6900 Heidelberg, West Germany
B Zwissler
K Messmer
Department of Anaesthesiology, University of Munich, Klinikum Grosshadern, Munich, West Germany
H Forst

Correspondence to: Dr Zwissler

Key words: pulmonary microembolism; right ventricle; preload; myocardial contraction; sonomicrometry; pressure-length loops

Submitted 31 July 1989
Accepted 1 November 1989

Preload on the right ventricle is known to influence its performance through the Frank-Starling mechanism.[1 2] In critically ill patients with high pulmonary vascular resistance (eg, in acute pulmonary embolism), the role of optimal right ventricular preload for preservation of stroke volume has been recognised.[3–7] Preload is usually defined as the tension or length of myocardial fibres at end diastole,[8] the two variables not being measurable under clinical conditions.[9] As a substitute, indices of right ventricular preload have been derived from measurements of central venous, right atrial, or right ventricular end diastolic pressures and, more recently, by assessing right ventricular filling volume or end diastolic dimensions.[10] However, all these variables are based on the assumption that changes in ventricular pressure or volume are paralleled by equivalent changes of myocardial end diastolic fibre length in all regions of the right ventricle.

The right ventricle is an irregular crescent shaped chamber surrounded by a concave free wall and a convex interventricular septum. It therefore seems likely that changes in end diastolic pressure or filling volume are not uniformly distributed within the ventricular lumen.[11 12] If this were true, changes in these variables would not necessarily reflect equivalent changes in myocardial end diastolic tension throughout the various regions of the right ventricular free wall. As a result, local contractile function of myocardial fibres would differ at different locations in the ventricular wall. To analyse this problem, local right ventricular preload and contraction pattern of myocardial segments were studied by means of sonomicrometry in two regions (inflow and outflow tract) of the canine right ventricular free wall, before and after acute pulmonary microembolisation.

Methods

The experiments were performed in accordance with the NIH guidelines on the care and use of laboratory animals. Thirteen fox hounds of either sex (weight 20.4±4.0 kg) were used. After premedication with propiomazin 1-1.5 $mg \cdot kg^{-1}$ (Combelen®, Bayer, Leverkusen, FRG), anaesthesia was induced by a bolus injection of pentobarbitone 20 $mg \cdot kg^{-1}$ (Nembutal®, Ceva, Segeberg, FRG), piritramid 0.75 $mg \cdot kg^{-1}$ (Dipidolor®, Janssen, Neuss, FRG) and alcuronium 0.25 $mg \cdot kg^{-1}$ (Alloferin®, Roche. Grenzach-Whylen, FRG) and maintained by continuous infusion of pentobarbitone 5 $mg \cdot kg^{-1} \cdot h^{-1}$. Additionally, a continuous infusion of piritramid 150 $\mu g \cdot kg^{-1} \cdot h^{-1}$ and alcuronium 75 $\mu g \cdot kg^{-1} \cdot h^{-1}$ was installed after termination of surgical preparation. For replacement of fluid losses, Ringer's solution 5 $ml \cdot kg^{-1} \cdot h^{-1}$ was administered throughout the experiment. A warming pad was used to keep core body temperature between 35.9 and 36.8°C. The dogs were intubated and mechanically ventilated at a rate of 12 $cycles \cdot min^{-1}$ at a tidal volume (V_T) of 15-18 $ml \cdot kg^{-1}$ using 100% O_2 (Servo Siemens C, Siemens-Elema, Solna, Sweden). V_T was adjusted to obtain an initial arterial P_{CO_2} between 4.7 and 5.3 kPa (35-40 mm Hg).

SURGICAL PREPARATION

Fluid filled catheters (PP270, Portex, Hythe, UK) were positioned in the descending aorta and superior vena cava via the left femoral artery and the right external jugular vein respectively. A thermistor tipped, flow directed catheter (Swan-Ganz, 7F, Edwards, Anasco, Puerto Rico) was inserted into the pulmonary artery via the right external jugular vein. Left ventricular pressure was measured by a tip manometer (PC 350, Millar Instruments, Houston, TX, USA) introduced via the right common carotid artery. After a right thoracotomy (5th intercostal space) and pericardiotomy, a second tip manometer was inserted into the right ventricle via an atrial stab incision. Thereafter, two pairs of miniaturised (external diameter 1.5-2 mm) piezoceramic ultrasonic transducers[13] were implanted in the longitudinal axis of the inflow tract and the outflow tract of the right ventricular free wall (fig 1). Each crystal was inserted via a stab incision and secured with an epicardial purse string suture (5-0 prolene®, Ethicon, Norderstedt, FRG). At the end of surgical preparation, the pericardium was sutured without constraint to the myocardium, after which the chest was closed air right, the lungs were reinflated and the remaining air removed by a chest drain.

EVALUATION OF METHODS

The implanted pressure transducers and their amplifying units were tested for stable zero and linearity of gain: drift was less than 0.13 kPa (1 mm Hg) at temperatures ranging from 34°-37°C and gain

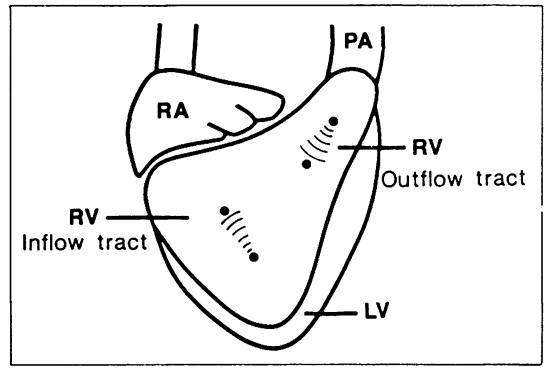

Figure 1 Ultrasonic crystals have been implanted in the longitudinal axes of the inflow and outflow tract of the right ventricular (RV) free wall. RA = right atrium; PA = pulmonary artery; LV = left ventricle.

was found linear up to 26.6 kPa (200 mm Hg). Prior to each experiment, the catheters (in a 36°C water bath) and amplifiers were prewarmed for at least 12 h and were calibrated immediately before use. After the end of the experiment, a second calibration was performed. The measured drift of electrical zero was less than 0.05 kPa (0.3 mm Hg) per hour. To prevent this drift from producing a significant error over a period of hours of low pressure measurement, a computerised drift correction was performed in every experiment (assuming linearity of drift between the first and last measurement).

MEASUREMENTS

All measurements were performed with the dogs in the left lateral position. Mean arterial and mean pulmonary artery pressure were recorded using Statham P23D6 transducers (Gould-Statham, Oxnard, CA, USA) referred to the right atrium and zeroed to atmospheric pressure. During data acquisition, phasic ventricular pressures, phasic contraction of myocardial segments and the ECG were sampled every 4 ms, digitised in real time (A/D Converter C1000, Cosima, Salem, OR, USA) and stored for subsequent evaluation using a PDP 11/03 computer system (DEC, Maynard, MA, USA). Data were analysed with interactive software developed in our laboratory. All signals were evaluated at end expiration using an average of three consecutive beats. We assessed mean, systolic and end diastolic pressures in the right and left ventricles. The rate of right ventricular pressure rise (dRVP/dt) was derived from the phasic right ventricular pressure curve by differentiation (Gould-Brush differentiator 13-4214-01, Cleveland, OH, USA). Cardiac output was obtained in triplicate by thermodilution technique (SP1435, Gould-Statham, Oxnard, CA, USA).

Arterial and mixed venous blood were analysed for P_{O_2}, P_{CO_2}, base excess and pH (ABL 3, Radiometer, Copenhagen, Denmark). CO_2 production per minute

($\dot{V}CO_2$) was measured by a CO_2 analyser 930 (Siemens-Elema, Solna, Sweden). Effective pulmonary compliance and expiratory resistance were assessed by a Lung Mechanics Calculator 940 (Siemens-Elema, Solna, Sweden) connected to the ventilator.

CALCULATIONS

The following haemodynamic and respiratory variables were calculated: cardiac index (CI) = $10 \cdot CO \cdot BW^{-0.75}$ (according to [14]); stroke index (SI) = $CI \cdot 1000 \cdot HR^{-1}$; and pulmonary vascular resistance (PVR) = $(PAP_{mean}\text{-}LVEDP) \cdot 79.9 \cdot CO^{-1}$; where CO = cardiac output, BW = body weight, HR = heart rate, PAP_{mean} = mean pulmonary artery pressure, and LVEDP = left ventricular end diastolic pressure.

Intrapulmonary shunt ($\dot{Q}_s/\dot{Q}_t$) was calculated as

$$\dot{Q}_s/\dot{Q}_t = (Cco_2 - Cao_2)/(Cco_2 - Cvo_2),$$

where $Cco_2 = Hb \cdot 1.39 + 0.0031 \cdot (P_B - 47 - Paco_2)$, $Cao_2 = (Hb \cdot 1.39 \cdot Sao_2)/100 + 0.0031 \cdot Pao_2$, and $Cvo_2 = (Hb \cdot 1.39 \cdot Svo_2)/100 + 0.0031 \cdot Pvo_2$. Cco_2, Cao_2 and Cvo_2 are O_2 contents in ideal (100% saturated) pulmonary capillary, systemic arterial and mixed venous blood, respectively. Hb is haemoglobin, P_B is barometric pressure, Pao_2 and $Paco_2$ (Pvo_2 and $Pvco_2$) are arterial (mixed venous) Po_2 and Pco_2, respectively. Sao_2 and Svo_2 are percent arterial and mixed venous O_2 saturation and were derived from the blood gas tensions according to the nomogram of Rossing and Cain.[15] The ratio of physiological dead space to tidal volume (V_D/V_T) was determined by the Enghoff modification of the Bohr equation as $V_D/V_T = (Paco_2\text{-}Peco_2) \cdot 100/Paco_2$, where $Peco_2$ (partial pressure of mean expiratory CO_2) was calculated as $Peco_2 = \dot{V}co_2 \cdot (P_B\text{-}47)/(V_T \cdot RR)$, $\dot{V}co_2$ being the CO_2 minute production. The alveolar gas equation was used to calculate alveolar-arterial O_2 difference ($AaDo_2$).

SONOMICROMETRY

Sonomicrometry provides an accurate description of the distance between two ultrasonic transducers.[16] Myocardial segment lengths were measured at end diastole (L_{dia}) and end systole (L_{sys}). End diastole was defined as the beginning of the upstroke of dRVP/dt, end systole as maximum negative dRVP/dt. Although true end systole is difficult to assess in the right ventricle, maximal negative dRVP/dt has been shown to reflect accurately the end of right ventricular ejection at normal and increased afterload.[17] Maximum and minimum segment length (L_{max}, L_{min}) were also determined. All length values were normalised by assuming segment length at end diastole in control to be 10 mm.[18] To quantify the pattern of local segment motion, the percentage of maximal (S_{max}), systolic (S_{sys}) and postsystolic fibre shortening (S_{psys}) as well as protosystolic elongation ("bulging") were defined as follows:

$$S_{sys} = (L_{dia}\text{-}L_{sys}) \cdot 100/L_{dia}$$
$$S_{max} = (L_{max}\text{-}L_{min}) \cdot 100/L_{max}$$
$$S_{psys} = (L_{sys}\text{-}L_{min}) \cdot 100/L_{sys}$$
$$\text{"bulging"} = (L_{max}\text{-}L_{dia}) \cdot 100/L_{dia}$$

To visualise the dynamics of right ventricular free wall contraction, pressure-length loops were constructed by plotting phasic changes of segment length against phasic changes of right ventricular pressure during one cardiac cycle by computer. Sonomicrometric data were obtained from 13 animals in the right ventricular inflow tract and from 12 animals in the right ventricular outflow tract.

EXPERIMENTAL PROTOCOL

After surgical preparation, the animals were isovolaemically haemodiluted with dextran 60 (Makrodex® 6%, Schiwa, Glandorf, FRG) to a packed cell volume of 30%. Packed cell volume was intentionally reduced to achieve identical baseline values of packed cell volume and haemoglobin concentration in all animals. The removed blood was used for replacement of blood samples taken for laboratory analyses during the experiment.

Following a stabilisation period of 30 min, control measurements were performed. Thereafter, the lungs were embolised by injection of a single dose of oleic acid (0.01 $ml \cdot kg^{-1}$) into the right atrium, followed by repetitive doses (0.5-1 g every 3-5 min; total 0.5 $g \cdot kg^{-1}$) of non-siliconised glass beads (diameter 100 μm) suspended and thoroughly mixed in 1-2 ml of dextran 60. Embolisation was interrupted when mean pulmonary artery pressure had increased by 10-15 mm Hg; 10 min later a second set of measurements was performed ($APME_1$). Thereafter, embolisation continued and was terminated when mean pulmonary artery pressure had reached a peak level of ≈40 mm Hg.[19] A third set of measurements was obtained 10 min after the end of acute pulmonary microembolisation ($APME_2$).

STATISTICAL ANALYSIS

Data are presented as means (SD) when normally distributed (haemodynamic variables, lung function); otherwise (sonomicrometry) the median and Q_1/Q_3 quartiles are given. Statistical evaluation was performed using SAS (5th edition, SAS Institute, Cary, MA, USA). A repeated measures analysis of variance (rANOVA) was used to test for the existence of an overall effect of the intervention (acute pulmonary microembolisation = APME) on a variable. In case of a significant F value ($p<0.05$) in the rANOVA, the following time points were compared by a paired *t* test (haemodynamic variables, lung function) or by Wilcoxon's signed rank test (sonomicrometry), respectively: $APME_1$ *v* control, $APME_2$ *v* $APME_1$, $APME_2$ *v* control. Differences were considered significant at $p<0.05$.

Results

HAEMODYNAMIC VARIABLES

The changes in haemodynamic variables induced by acute pulmonary microembolisation are shown in table I. According to the protocol, embolisation was interrupted when pulmonary artery pressure had increased by 10-15 mm Hg ($APME_1$). At this time, there was a 3.5-fold rise in pulmonary vascular resistance and a significant 30% increase in mean and systolic right ventricular pressure, while end diastolic right ventricular pressure remained unchanged. In contrast, left ventricular end diastolic pressure had decreased, accompanied by a slight fall in mean left ventricular and aortic pressures. Despite a reduced stroke index, cardiac index was maintained as a result of a rise in heart rate. At peak pulmonary artery pressure ($APME_2$), right ventricular end diastolic pressure had slightly but significantly increased as compared to control and $APME_1$. Pulmonary vascular resistance and right ventricular systolic and mean pressure had reached a maximum, while end diastolic and mean left ventricular pressure as well as mean aortic pressure continued to decrease. Despite the lower stroke index, no depression of cardiac index was observed due to further increase of heart rate.

LUNG FUNCTION

Changes in lung function and blood gases induced by acute pulmonary microembolisation are shown in table II. Lung mechanics (compliance, resistance) and gas exchange (Pa_{O_2}, alveolar-arterial O_2 difference, shunt, dead space) had deteriorated at $APME_1$ and even more at $APME_2$. Embolisation resulted in hypercapnia and respiratory acidosis at $APME_2$.

SONOMICROMETRY

Right ventricular segment lengths — Table III summarises the data of local segment lengths before

Table I Changes in haemodynamic variables after pulmonary microembolism. Results are means (SD).

	Control	Pulmonary microembolism	
		$APME_1$	$APME_2$
HR (beats·min^{-1})	104(26)	117(22)***	140(23)***†††
CI (litre·min^{-1}·BW$^{-0.75}$)	4.0(4.0)	3.8(0.4)	4.1(0.6)
SI (ml·BW$^{-0.75}$)	40(9)	34(6)***	30(6)*†††
RV pulmonary haemodynamics			
PAP_{mean} (mm Hg)	11(2)	22(2)	39(4)
PVR (Pa·litre^{-1}·min)	175(97)	617(145)***	1221(445)***†††
RVP_{mean} (mm Hg)	9(3)	13(3)***	23(5)***†††
RVP_{sys} (mm Hg)	24(4)	32(6)***	48(9)***†††
RVEDP (mm Hg)	4.0(3.3)	4.5(2.5)	5.7(3.2)*†
LV systemic haemodynamics			
MAP_{mean} (mm Hg)	106(15)	96(17)***	85(17)**†††
LVP_{mean} (mm Hg)	43(7)	40(6)***	39(8)††
LVEDP (mm Hg)	5.5(2.3)	4.0(2.0)***	3.3(2.0)††

$APME_1$=measurements made after microembolisation caused mean pulmonary artery pressure (PAP_{mean}) to increase by 10-15 mm Hg; $APME_2$=measurements made when PAP_{mean} reached ≈ 40 mm Hg; HR=heart rate; SI=stroke index; CI=cardiac index; PVR=pulmonary vascular resistance; RVP_{mean}=mean right ventricular (RV) pressure; RVP_{sys}=systolic RV pressure; RVEDP=end diastolic RV pressure; MAP_{mean}=mean arterial pressure; LVP_{mean}=mean left ventricular (LV) pressure; LVEDP=end diastolic LV pressure.
*p<0.05, **p<0.01, ***p<0.001 ($APME_1$ *v* control, $APME_2$ *v* $APME_1$); †p<0.05, ††p<0.01, †††p<0.001 ($APME_2$ *v* control). No statistical test was performed on PAP_{mean} because this variable was intentionally changed by microembolisation.

Table II Changes in lung function after pulmonary microembolism. Results are means (SD).

	Control	Pulmonary microembolism	
		$APME_1$	$APME_2$
Lung mechanics			
C_{eff} (ml·kPa^{-1})	386(65)	355(79)*	315(59)***†††
R_{exp} (kPa·s·litre^{-1})	1.07(0.09)	1.19(0.19)*	1.30(0.17)***†††
Gas exchange			
Pa_{O_2} (kPa)	74.9(5.9)	70.4(7.6)***	49.1(18.5)***†††
Pa_{CO_2} (kPa)	5.1(0.3)	5.4(0.4)***	6.5(0.8)***†††
AaD_{O_2} (kPa)	14.8(5.6)	19.6(7.3)***	42.1(18.5)***†††
Q_s/Q_t (%)	9(4)	12(5)**	22(10)**†††
V_D/V_T (%)	51(4)	54(5)**	66(8)***†††
Acid base status			
pH	7.32(0.02)	7.30(0.02)**	7.23(0.04)***†††
BE (mmol·litre^{-1})	−5.8(1.3)	−5.9(0.9)	−6.9(1.2)**††

C_{eff}=effective pulmonary compliance; R_{exp}=expiratory resistance; Pa_{O_2}=partial pressure of arterial oxygen; Pa_{CO_2}=partial pressure of arterial CO_2; AaD_{O_2}=alveolar-arterial oxygen difference; Q_s/Q_t=intrapulmonary shunt; V_D/V_T=physiological dead space, BE=base excess. See table I for other abbreviations.
*p<0.05, **p<0.01, ***p<0.001 ($APME_1$ *v* control, $APME_2$ *v* $APME_1$); †p<0.05, ††p<0.01, †††p<0.001 ($APME_2$ *v* control).

Table III Changes in right ventricular segment lengths after pulmonary microembolism. Results are median (Q_1/Q_3 quartiles).

	Control	Pulmonary microembolism	
		$APME_1$	$APME_2$
Inflow tract (n=13)			
L_{dia} (mm)	10.0	10.1* (10.0-10.2)	10.3**†† (10.1-10.5)
L_{max} (mm)	10.2 (10.1-10.3)	10.3* (10.2-10.5)	10.5**†† (10.4-10.6)
L_{sys} (mm)	9.4 (9.0-9.8)	9.7** (9.2-9.9)	9.8**†† (9.4-10.2)
L_{min} (mm)	9.2 (9.0-9.6)	9.6** (9.1-9.8)	9.6†† (9.4-9.9)
Outflow tract (n=12)			
L_{dia} (mm)	10.0	9.7** (9.6-9.9)	9.6† (9.5-9.9)
L_{max} (mm)	10.1 (10.0-10.2)	9.8 (9.7-10.3)	9.9 (9.5-10.5)
L_{sys} (mm)	8.8 (8.5-9.4)	9.0** (8.5-9.8)	9.2†† (8.8-10.1)
L_{min} (mm)	8.5 (8.2-9.1)	8.7 (8.3-9.1)	8.9 (8.5-9.3)

L_{dia}=end diastolic segment length (SL), L_{max}=maximal SL, L_{sys}=end systolic SL, L_{min}=minimal SL. For other abbreviations see table I.
*p<0.05. **p<0.01 ($APME_1$ *v* control, $APME_2$ *v* $APME_1$); †p<0.05, ††p<0.01 ($APME_2$ *v* control).

and after acute pulmonary microembolisation. In the right ventricular inflow tract end diastolic length (L_{dia}) was increased at $APME_1$ and $APME_2$, while in the outflow tract it decreased significantly. This finding is shown most clearly in fig 2, where control values of end diastolic length are depicted with the values at $APME_2$ for each experiment. In the right ventricular inflow tract, end diastolic length did not change in two experiments, but was increased in 11. In contrast, end diastolic length in the outflow tract was considerably decreased in 10 of 12 animals.

When maximal segment length (L_{max}) was analysed in place of end diastolic length, similar results were obtained (table III, fig 2). Maximal segment length in the right ventricular inflow tract was increased at $APME_2$ in all experiments, whereas in the outflow tract it declined in nine of 12 animals.

While end diastolic and maximal segment lengths were affected differently by pulmonary microembolism in the right ventricular inflow and outflow tracts, changes in systolic and minimal segment length were found to be similar, ie, systolic and minimal length significantly and equivalently increased subsequent to embolisation in both regions of the right ventricular free wall (table III).

Right ventricular segment shortening — Table IV (pooled data) and fig 3 (single experiments) show that systolic and maximal shortening were not significantly altered by acute pulmonary microembolisation in the right

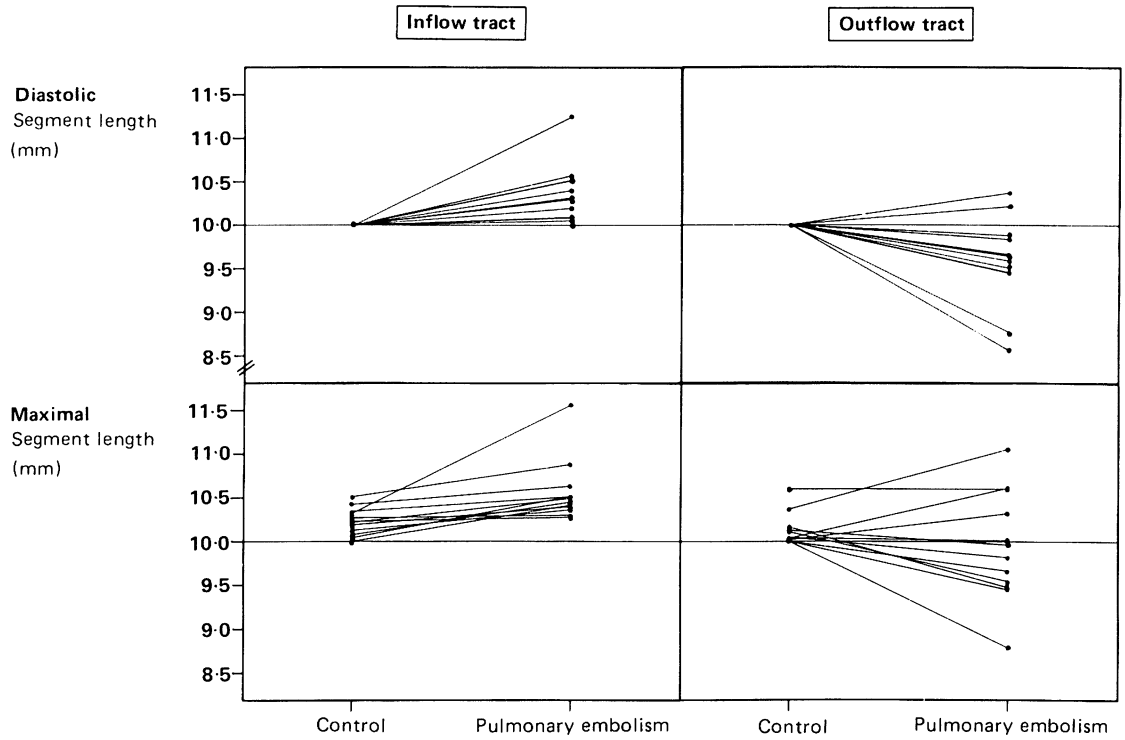

Figure 2 For each experiment, end diastolic and maximal myocardial segment length in the right ventricular inflow and outflow tracts have been compared before (control) and after acute pulmonary microembolism (≙$APME_2$, see table I for explanation).

Table IV Changes in right ventricular segment shortening after pulmonary microembolism. Results are median (Q_1/Q_3 quartiles).

	Control	Pulmonary microembolism	
		$APME_1$	$APME_2$
Inflow tract (n=13)			
S_{sys} (%)	5.9 (2.3-9.9)	5.6 (2.3-8.8)	6.7 (0.1-8.0)
S_{max} (%)	9.2 (6.7-11.9)	8.6 (6.0-11.4)	8.1 (6.0-10.8)
S_{psys} (%)	1.1 (0.1-1.7)	0.8 (0.7-2.0)	1.7 (0.6-2.7)
"bulging" (%)	2.2 (1.0-3.3)	2.3 (1.1-3.0)	2.8 (0.8-3.3)
Outflow tract (n=12)			
S_{sys} (%)	11.6 (5.8-15.1)	8.3** (0.5-11.7)	2.7**†† (-2.9-6.4)
S_{max} (%)	15.0 (9.3-18.0)	13.0* (9.7-14.8)	10.8*† (8.7-11.7)
S_{psys} (%)	1.3 (0.7-3.7)	2.6 (1.3-4.1)	4.6 (1.9-6.3)
"bulging" (%)	0.4 (0.0-1.5)	1.3* (0.6-4.9)	2.5*†† (0.6-7.1)

S_{sys}=systolic shortening of the myocardial segment; S_{max}=maximal segment shortening; S_{psys}=postsystolic segment shortening; "bulging"=protosystolic segment elongation. For other abbreviations see table I.
*p<0.05, **p<0.01 ($APME_1$ *v* control, $APME_2$ *v* $APME_1$); †p<0.05, ††p<0.01 ($APME_2$ *v* control).

ventricular inflow tract. The unchanged amplitude of contraction results from an equal rise of systolic (minimal) and diastolic (maximal) segment length (see above). In contrast, a significant fall in systolic and maximal shortening subsequent to microembolisation was observed in the right ventricular outflow tract, originating from lowered diastolic (maximal) segment length in the presence of increased systolic (minimal) length. As seen in fig 3, microembolisation reduced the amplitude of local outflow tract contraction in all experiments.

In both regions of the right ventricular free wall, paradoxical systolic elongation (≙ negative systolic shortening) was absent at control, but present in three (inflow tract) and four (outflow tract) animals as a result of the microembolisation (fig 3). There was no difference in the extent of postsystolic shortening in the two regions before and after microembolisation. However "bulging" was found at any level of microembolisation in the right ventricular outflow tract, but not in the inflow tract. It should be noted that the degree of "bulging" was different in the two regions at control (table IV) and that microembolisation eliminated this difference by increasing "bulging" in outflow tract without affecting the inflow tract.

Right ventricular pressure-length loops — Pressure-length loops of right ventricular inflow and outflow tracts from four experiments are shown in fig 4. While

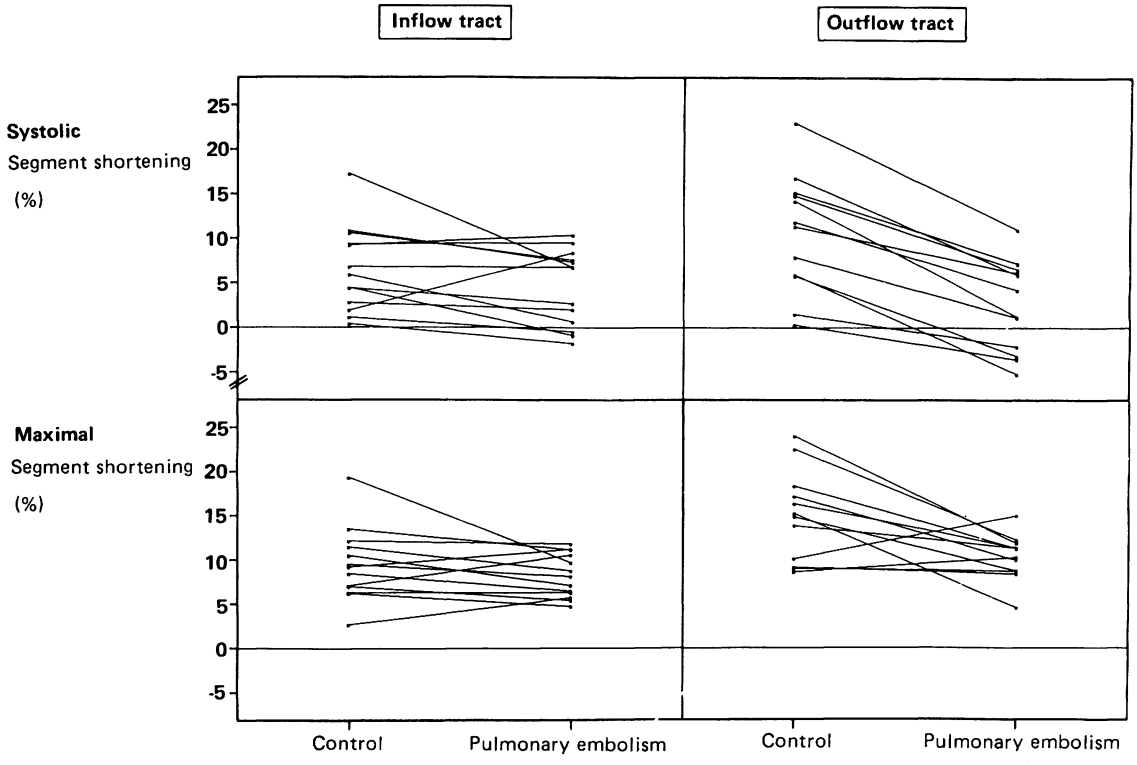

Figure 3 For each experiment, systolic and maximal myocardial segment shortening in the right ventricular inflow and outflow tracts have been compared before (control) and after acute pulmonary microembolism (≙$APME_2$, see table I for explanation).

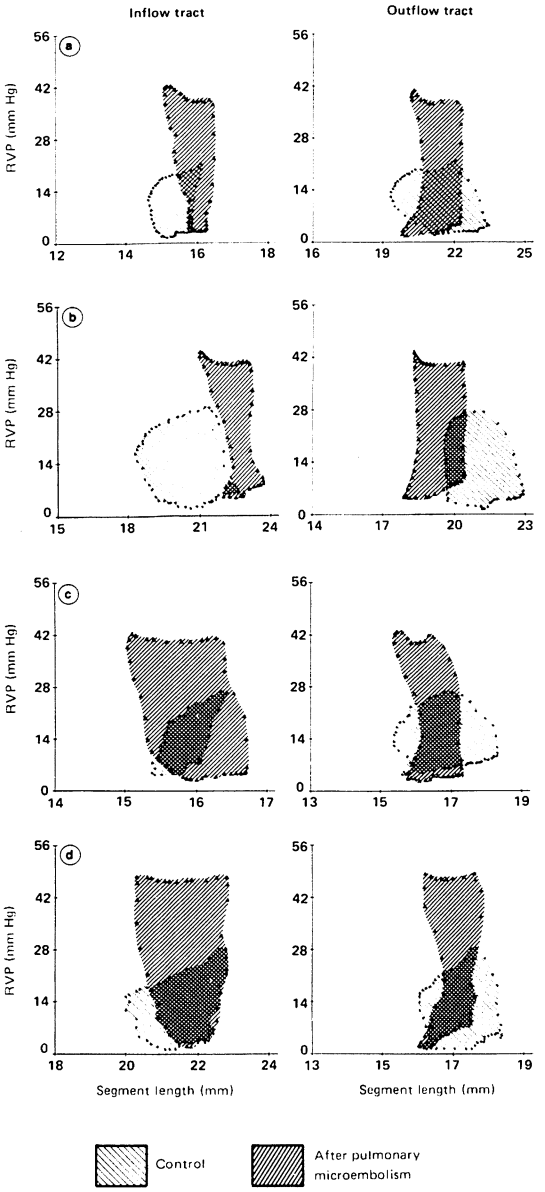

Figure 4 Pressure-length loops from segments of the right ventricular inflow tract (left graphs) and outflow tract (right graphs) have been constructed for four experiments (a-d) before and after acute pulmonary microembolism (≙$APME_2$, see table I for explanation). Embolisation resulted in a shift to the right (or no shift in d) of loops from the inflow tract. In contrast, loops from the outflow tract were shifted to the left (for further details see Results).

at control, the loops were found to be triangular or oval in shape, they became rectangular after pulmonary embolism ($APME_2$). No major differences in these qualitative changes of the dynamic contraction pattern were observed between the inflow and outflow tracts. However, the segment length at which the steep rise of right ventricular pressure occurred (≙ L_{dia}), was influenced differently by microembolisation: within the same experiment, end diastolic segment length was increased or remained unchanged in the right ventricular inflow tract, but declined in the outflow tract (fig 4). Consequently, the loops were shifted to the right in the inflow tract or to the left in the outflow tract. Segment shortening was decreased (fig 4b), unaffected (fig 4a,d) or increased (fig 4c) in the inflow tract, while shortening in the outflow tract worsened in all experiments. Figures 4b and 4d suggest that a dissociation of end diastolic pressure and end diastolic segment length may occur in the right ventricular outflow tract subsequent to acute microembolisation: while the end diastolic pressure increased, end diastolic length considerably decreased in these experiments.

Discussion

The inflow tract and outflow tract of the right ventricle are known to differ with respect to origin, morphology, innervation and function.[16 20–24] For these reasons, changes of local myocardial fibre lengths and local contraction pattern have been assessed after pulmonary microembolisation separately in both regions of the right ventricular free wall. It was our aim to determine whether the myocardial fibres of the right ventricular free wall respond uniformly to an acute increase in right ventricular afterload. Studies addressing this topic in the past[16 25 26] have been performed in pericardectomised, open chest dogs[16 25] and most often pulmonary hypertension was induced by mechanical narrowing of the pulmonary artery.[16 26] These experimental settings, however, do not adequately reflect the clinical situation[27 28] of patients presenting with a closed chest/pericardium and pulmonary hypertension due to microvascular injury rather than to pulmonary constriction.[29 30]

In the present study, pericardium and chest were closed after surgery and right ventricular afterload was increased by acute microembolisation of the lungs resulting in profound changes in pulmonary function. The decrease of Pa_{O_2} and effective pulmonary compliance and the increase of $AaDo_2$, $\dot{Q}_s/\dot{Q}_t$, Pa_{CO_2}, and V_D/V_T indicate the development of ventilation-perfusion ($\dot{V}/\dot{Q}$) mismatch, increased dead space ventilation, an increase in intrapulmonary shunt and interstitial oedema. Similar findings have been reported in patients with pulmonary embolism.[29] Hence this study is the first to measure the local response of the right ventricular free wall to increased right ventricular afterload in a "physiological setting".

Embolisation was terminated at a peak pulmonary artery pressure of 40 mm Hg in order to avoid global cardiac failure.[31] As a result, cardiac index remained unchanged during the whole study (table I) allowing measurements to be made in stable haemodynamic conditions.

CONTRACTION PATTERN OF THE RIGHT VENTRICLE

Segment lengths and local preload

The main finding in our experiments was that acute pulmonary microembolisation resulted in divergent changes in end diastolic fibre lengths depending upon the region in the myocardium: while end diastolic length was increased by microembolisaton in the right ventricular inflow tract, it was decreased in the outflow tract. Since the end diastolic fibre length is a preferred and valid measure of preload in either ventricle,[8 9] our results suggest that acute pulmonary microembolisation induces regionally different changes in local preload within the canine right ventricular free wall.

In closed chest dogs, Santamore *et al*[26] have investigated the influence of increased right ventricular afterload on end diastolic segment length in both the inflow and outflow tracts of the right ventricle. As in the present study, end diastolic length in the inflow tract was found to be increased after pulmonary artery constriction. These authors did, however, observe that end diastolic segment length was unchanged in the outflow tract, in contrast to our present results. This may be explained by the higher right ventricular afterload in Santamore's study. This view would explain our finding that the two animals in which the outflow tract segment length had increased were those reaching the highest level of pulmonary hypertension after embolisation. On the other hand, segment length was found to be already reduced in the outflow tract at $APME_1$, suggesting that a decrease in segment length only occurs at moderate levels of pulmonary hypertension, while at a high pulmonary artery pressure the outflow tract becomes redistended.

Several sources of error have to be considered when assessing end diastolic segment length. As in other studies,[16 25 32] end diastole has been defined for both regions as the beginning of the upstroke of dRVP/dt. Under normal conditions, relaxation of the right ventricular inflow tract precedes relaxation of the outflow tract;[10 23 26] to rule out the possibility that incomplete relaxation of the outflow tract (ie, underestimation of true end diastolic segment length in comparison with the inflow tract) has influenced our results, we have additionally analysed maximal segment length. Since changes of diastolic and maximal lengths diverged in one experiment only (fig 2), a systematic error in assessing end diastolic length at the beginning of dRVP/dt upstroke can be excluded.

In order not to compromise the ability of the heart to adapt to acute pulmonary microembolisation and so as not to alter the physiological time course of right ventricular electrical activation[33] and contraction,[16] heart rate was not controlled. The increase in heart rate by 35% at $APME_2$ might therefore have caused incomplete relaxation of the right ventricular outflow tract and thereby a decrease of segment length in this region. Since, however, all measurements were performed simultaneously, changes in heart rate should have affected segment length in the same way in both regions of the right ventricular free wall. Thus tachycardia is not likely to explain the opposite changes of end diastolic segment length in the inflow and outflow tracts.

Segment shortening

The ultrasonic crystals were implanted in the longitudinal axis of the inflow and outflow tracts because in this direction segment shortening is maximum in both regions.[28] At control, maximal shortening was 15.0% in the outflow tract and 9.2% in the inflow tract. Higher values have been described in open chest dogs by Raines *et al*[23] (21% and 13%, respectively), Priebe[25] (19.6% and 18.9%) and Morris *et al*[17] (21% in the inflow tract). Because segment movement is increased in pericardectomised hearts[28] the former results cannot be compared directly with the present findings. However, our results compare favourably with data obtained by means of implanted radio-opaque markers in anaesthetised, closed chest dogs: Meier *et al*[28] reported segment shortening to be 12.2% in the right ventricular outflow tract and 11.7% in the inflow tract of acutely instrumented dogs. Slightly higher values (16.1% and 13.8%, respectively) have been found by Santamore *et al* in chronically instrumented dogs.[26]

Our results provide evidence that segment shortening is affected differently by acute pulmonary microembolisation in right ventricular inflow and outflow tracts. While shortening was not affected in the inflow tract, it decreased in the outflow tract. Since the degree of right ventricular free wall shortening is a linear function of end diastolic segment length[2] the decrease in outflow tract shortening could be explained by the concurrent fall in end diastolic segment length. The functional consequence of the discrepancy in inflow tract and outflow tract shortening is emphasised by the fact that with an increased end diastolic segment length, less shortening is needed to eject the identical volume. Therefore, outflow tract contraction substantially decreased not only with respect to absolute amplitude of contraction but even more so with regard to efficiency of contraction. In contrast, inflow tract contraction — starting from an increased end diastolic segment length — has presumably been more efficient in microembolisation as compared to control despite unchanged systolic shortening.

These results are supported by the work of Morris *et al*,[17] who could not show a substantial decrease in inflow tract shortening subsequent to pulmonary artery constriction in open chest dogs. Accordingly, in a similar model of pulmonary artery constriction in closed chest dogs, Santamore *et al*[26] reported shortening to be decreased in the outflow tract without being significantly altered in the inflow tract.

However, due to the peristaltic pattern of right

ventricular free wall contraction,[24] care has to be taken when systolic segment shortening in the inflow and outflow tracts is compared directly. According to Priebe,[25] we assessed systolic shortening at exactly the same time (peak negative dRVP/dt) in both the inflow tract and the outflow tract and calculated systolic segment shortening as end diastolic minus systolic segment length. Since the right ventricular outflow tract is known to shorten and to lengthen later than the inflow tract,[24] this technique may underestimate active contraction of the outflow tract as compared to the inflow tract. In order to evaluate this potential source of error, right ventricular outflow tract shortening has been recalculated by subtracting minimal segment length (instead of systolic segment length) from end diastolic segment length: outflow tract shortening was now found to be 14.8%, 11.3% and 6.5% at control, $APME_1$ and $APME_2$ respectively ($p<0.01$ between each measurement), and was thus $\approx 3\%$ higher than if calculated as end diastolic minus systolic segment length (see table IV). However, there were no major differences with respect to the absolute changes of outflow tract shortening subsequent to microembolisation and no difference with respect to the levels of significance. This suggests that our finding of a decreased outflow tract contraction due to microembolisation holds true independent of the method used for calculation of systolic outflow tract shortening.

No definite explanation can be given at the moment as to the mechanisms causing the regionally opposite changes in local right ventricular preload and segment shortening after microembolisation. The well known disparity between the right ventricular inflow and outflow tracts with respect to fibre architecture[20] and fibre compliance[8] might account for quantitatively different changes in diastolic segment length, but hardly explains opposite changes of local preload within the right ventricular free wall following microembolisation. Since functional signs of right ventricular inflow tract ischaemia were not observed (eg, reduced segment shortening, protosystolic segment elongation), it seems unlikely that the increase in the end diastolic fibre length after microembolisation was caused by ischaemic myocardial dilatation.

It seems more likely that the inhomogeneous sympathetic innervation of the right ventricular free wall[11 20 34] and the resulting regionally different degrees of sympathetic activation of right ventricular myocardium have been responsible for the discrepant changes in local preload and local segment shortening in the inflow and outflow tracts subsequent to microembolisation.

Dynamic pattern of right ventricular contraction (PL loops)

As previously described,[1 2] the configuration of the right ventricular pressure-length loops was found to be oval or triangular under control conditions. After acute pulmonary microembolisation, loops assumed a rectangular shape with peak right ventricular pressure coinciding with minimum segment length (fig 4). Since inflow tract shortening is closely correlated with changes of right ventricular volume,[2 35] right ventricular ejection obviously does not continue beyond peak right ventricular pressure when afterload is elevated. Thus in acute pulmonary microembolisation right ventricular dynamic contraction very much resembles left ventricular contraction.[2 18]

As an explanation of this phenomenon, an "activation" of the Starling mechanism subsequent to increased right ventricular free wall distension has been proposed.[36] In the present study, however, rectangular PL loops occurred not only in the inflow tract, but also in the outflow tract despite end diastolic segment length being reduced by microembolisation in this region. This indicates that mechanisms other than increased local preload (eg, sympathoadrenergic stimulation) have caused the outflow tract contraction pattern after microembolisation to resemble the normal left ventricular contraction pattern.

CLINICAL IMPLICATIONS

The tenet that fibre tension is equally affected throughout the myocardial wall by changes in afterload does not apply for the right ventricle after acute pulmonary microembolisation because regionally divergent changes of local right ventricular preload have been encountered within the right ventricular free wall.

This finding has consequences for the interpretation of global measures of right ventricular preload. In the schematic cross section of the heart (fig 5), the diastolic segment length of the right ventricular inflow and outflow tracts is indicated by the distance of the ultrasonic crystals. The diagram on the left depicts the right ventricle in its normal configuration. In pulmonary embolism (diagram on the right), the reduction in diastolic segment length in the outflow

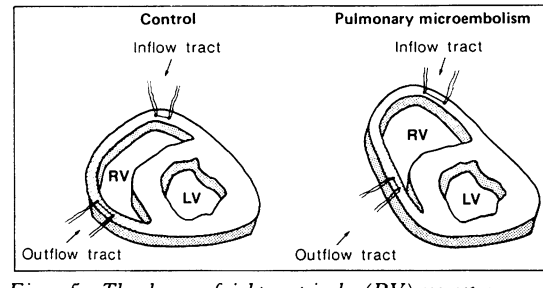

Figure 5 The change of right ventricular (RV) geometry following pulmonary microembolism is shown in this scheme of a cross section of the heart (for further explanation see Discussion).

tract coincides with a dilatation of the inflow tract and thereby results in an altered configuration of the right ventricle. Comparison of the graphs reveals, however, that the change in right ventricular geometry is not necessarily accompanied by a change in end diastolic volume. Nevertheless, the functional state of the myocardial fibres may have improved or worsened considerably in this situation.

Our findings may have implications for the clinical evaluation of right ventricular function in patients presenting with an acute increase in pulmonary vascular resistance. First, global right ventricular performance may be altered in these patients as a result of a change in right ventricular geometry despite unchanged end diastolic volume. Second, right ventricular inflow tract dilatation may already be present without being reflected by a high end diastolic volume. In these patients, even a minor increase in end diastolic volume could result in acute overdistension of the inflow tract and thereby depress global right ventricular performance and cardiac output.

Third, when estimating right ventricular end diastolic volume by echocardiographic measurement of the septal to right ventricular free wall distance, the direction of the ultrasonic beam has to be taken into account: depending on whether septal to inflow tract or septal to outflow tract distance is assessed, a different end diastolic volume may be calculated if acute pulmonary hypertension is present. It should be noted, however, that our results apply to the intact right ventricle; the effects of pulmonary microembolisation on a compromised right ventricular myocardium might be more pronounced and remain to be clarified.

CONCLUSION

In conclusion, our study has shown substantial differences between the inflow and outflow tract of the primarily intact canine right ventricle with regard to changes in local preload and segment shortening induced by pulmonary microembolisation. Indices of global right ventricular preload do not reflect these local differences and therefore may be misinterpreted. Regardless of the opposite changes of local preload, however, similar changes in the dynamic pattern of contraction (PL loops) occur in both regions following acute pulmonary microembolisation: the triangular or oval PL loops become rectangular in shape, indicating that under conditions of an acutely elevated right ventricular afterload, the local dynamic contraction of both the inflow tract and the outflow tract closely resembles the contraction pattern of the left ventricle.

The authors thank Roswitha Schwarz, Jutta Schulte, Karin Sonnenberg and Heidrun Voigt for their expert technical assistance and Dr sc hum Heinrich Zeintl for developing the computer evaluation system.

This work was supported by Deutsche Forschungsgemeinschaft grant SFB 320/C3.

1 Maughan WL, Shoukas AA, Sagawa K, Weisfeldt ML. Instantaneous pressure-volume relationship of the canine right ventricle. *Circ Res* 1979;**44**:309–15.
2 Morris JJ, Pellom GL, Murphy CE, Salter DR, Goldstein JP, Wechsler AS. Quantification of the contractile response to injury: assessment of the work length relationship in the intact heart. *Circulation* 1987;**76**:717–27.
3 Brunet F, Dhainaut JF. Right ventricular performance during mechanical ventilation in ARDS. In: Vincent JL, ed. *Update in intensive care and emergency medicine*, vol 5. Berlin: Springer, 1988:219–26.
4 Qvist J, Mygind T, Crottogini A, *et al*. Cardiovascular adjustments to pulmonary vascular injury in dogs. *Anesthesiology* 1988;**68**:341–9.
5 Sibbald WJ, Driedger AA, Myers ML, Short AIK, Wells GA. Biventricular function in the adult respiratory distress syndrome. Hemodynamic and radionuclide assessment with special emphasis on right ventricular function. *Chest* 1983;**84**:126–34.
6 Weber KT, Janicki JS, Shroff SG, Likoff MJ, Sutton MGJ. The right ventricle: physiologic and pathophysiologic considerations. *Crit Care Med* 1983;**11**:323–8.
7 Dhainaut JF, Brunet F, Villemant D. Monitoring of right ventricular performance in the ICU. In: Vincent JL, ed. *Update in intensive care and emergency medicine*, vol 3. Berlin: Springer, 1987:336–41.
8 Leyton RA, Spotnitz HM, Sonnenblick EH. Cardiac ultrastructure and function: sarcomeres in the right ventricle. *Am J Physiol* 1971;**221**:902–10.
9 Sibbald WJ, Driedger AA. Right ventricular function in acute disease states: pathophysiological considerations. *Crit Care Med* 1983;**11**:339–45.
10 Hurford WE, Zapol WM. The right ventricle and critical illness: a review of anatomy, physiology, and clinical evaluation of its function. *Intensive Care Med* 1988;**14**:448–57.
11 Pace JB, Keefe WF, Armour JA, Randall WC. Influence of sympathetic nerve stimulation on right ventricular outflow-tract pressures in anesthetized dogs. *Circ Res* 1969;**24**:397–407.
12 Pinsky MR. Assessment of right ventricular function in the critically ill: fact, fancy, and perspectives. In: Vincent JL, ed. *Update in intensive care and emergency medicine*, vol 8. Berlin: Springer, 1989:518–23.
13 Heimisch W, Hagl S, Gebhardt K, Meisner H, Mendler N, Sebening F. Direct measurement of cyclic changes in regional wall geometry in the left ventricle of the dog. *Innov Tech Biol Med* 1981;**2**:487–501.
14 Holt JP, Rhode EA, Kines H. Ventricular volumes and body weight in mammals. *Am J Physiol* 1968;**215**:704–15.
15 Rossing RG, Cain SM. A nomogramm relating PO_2, pH, temperature and hemoglobin saturation in the dog. *J Appl Physiol* 1966;**21**:195–201.
16 Pouleur H, Lefevre J, van Mechelen H, Charlier AA. Free-wall shortening and relaxation during ejection in the canine right ventricle. *Am J Physiol* 1980;**239**:601–13.
17 Morris JJ, Pellom GL, Hamm DP, Everson CT, Wechsler AS. Dynamic right ventricular dimension. Relation to chamber volume during the cardiac cycle. *J Thorac Cardiovasc Surg* 1986;**91**:879–87.
18 Akaishi M, Weintraub WS, Schneider RM, Klein LW, Agarwal JB, Helfant RH. Analysis of systolic bulging. Mechanical characteristics of acutely ischemic myocardium in the conscious dog. *Circ Res* 1986;**58**:209–17.
19 Zwissler B, Forst H, Ishii K, Messmer K. A new experimental model of ARDS and pulmonary hypertension in the dog. *Res Exp Med* 1989;**189**:427–38.
20 Armour JA, Pace JB, Randall WC. Interrelationship of architecture and function of the right ventricle. *Am J Physiol* 1970;**218**:174–9.
21 Keith A. Fate of the bulbus cordis in the human heart. *Lancet* 1924;ii:1267–73.
22 March HW, Ross JK, Lower RR. Observations on the behavior of the right ventricular outflow tract, with reference to its developmental origins. *Am J Med* 1962;**32**:835–45.
23 Raines RA, LeWinter MM, Covell JW. Regional shortening patterns in canine right ventricle. *Am J Physiol* 1976;**231**:1395–400.
24 Foex P. Right ventricular contraction. In: Vincent JL, ed. *Update in intensive care and emergency medicine*, vol 3. Berlin: Springer, 1987:72–80.
25 Priebe HJ. Efficacy of vasodilator therapy in canine model of acute pulmonary hypertension. *Am J Physiol* 1988;**255**:1232–9.

26 Santamore WP, Meier GD, Bove AA. Effects of hemodynamic alterations on wall motion in the canine right ventricle. *Am J Physiol* 1979;**236**:254–62.
27 Calvin JE, Baer RW, Glantz SA. Pulmonary artery constriction produces a greater right ventricular afterload than lung microvascular injury in the open chest dog. *Circ Res* 1985;**56**:40–56.
28 Meier GD, Bove AA, Santamore WP, Lynch PR. Contractile function in canine right ventricle. *Am J Physiol* 1980;**239**:794–804.
29 Moser KM. Pulmonary embolism: state of the art. *Am Rev Respir Dis* 1977;**115**:829–52.
30 Zapol WM, Snider MT. Pulmonary hypertension in severe acute respiratory failure. *N Engl J Med* 1977;**296**:476–80.
31 Hurford WE, Barlai-Kovach M, Strauss HW, Zapol WM, Lowenstein E. Canine biventricular performance during acute progressive pulmonary microembolization: regional myocardial perfusion and fatty acid uptake. *J Crit Care* 1987;**2**:270–81.
32 Forst H, Racenberg J, Messmer K. Lokale und globale Kontraktilität des rechten Ventrikels bei Ischämie seiner freien Wand. *Anaesthesist* 1988;**37**:356–65.
33 Freud GE, Stern MC, Watson H, Durrer D. Activation of the hypertrophic right ventricle in the dog. *Cardiovasc Res* 1975;**9**:302–13.
34 Tobin JR, Blundell PE, Goodrich RG, Swan HJC. Induced pressure gradients across infundibular zone of right ventricle in normal dogs. *Circ Res* 1965;**16**:162–73.
35 Hamm DP, Everson CT, Freedman BM, Pellom GL, Christian C, Wechsler AS. The passive right ventricular volume-dimension relationship in the isolated canine heart. *Surg Forum* 1984;**35**:266–8.
36 Piene H, Covell JW. Local auxotonic systolic force and work in canine right ventricular free wall. *Am J Physiol* 1983;**244**:186–93.